Desalination and Water Treatment
www.deswater.com
doi: 10.5004/dwt.2023.29740

303 (2023) 193–199
August

Assessment, characterization, and separation of Alizarin red dye from aqueous solution using M-Fe layered double hydroxide

Hossam F. Nassar[a,*], Hussein M. Ahmed[b], Mariam E. Fawzy[c]

[a]*Environmental Science and Industrial Development Department, Faculty of Postgraduate Studies for Advanced Sciences, Beni-Suef University, 62511 Beni-Suef, Egypt, email: hossamnassarnrc@gmail.com*
[b]*Housing and Building Research Center (HBRC), Sanitary and Environmental Engineering Institute (SEI), Egypt, email: hussein_fee@yahoo.com*
[c]*Water Pollution Research Department, National Research Centre, P.O. Box: 12622, Dokki, Giza, Egypt, email: mariamemadeldin@hotmail.com*

Received 7 January 2023; Accepted 20 June 2023

ABSTRACT

Recently, layered double hydroxides (LDH) have been applied intensively and attracted tremendous attention due to their flexible chemical composition and physical properties. In this study, we prepared a series of M (Mg and Zn)-Fe LDH at different conditions using the co-precipitation method. The influence of several important parameters was studied including M (Mg and Zn):Fe molar ratio, M-Fe LDH concentration, and pH. In this work, the potentialities of both synthesized adsorbents of M (Mg and Zn)-Fe LDH for the separation of cationic Alizarin red dye (ARD) from aqueous solutions were studied. The obtained results investigated that the maximum separation efficiency of 20 mg/L ARD was achieved at the molar ratio (4:1) of both adsorbents M (Mg and Zn):Fe at pH 6.0 and room temperature. Both pseudo-second-order kinetic models of Langmuir and Freundlich were successfully applied for the adsorption of ARD on both M (Mg and Zn)-Fe LDH adsorbents. By comparing the q_m values for both adsorbents, we obtained that Mg-Fe LDH had a significantly higher adsorption capacity of 72.4 mg/g than that obtained from Zn-Fe LDH of 33.8 mg/g. These results indicated that Mg-Fe LDH has better adsorption efficiency than Zn-Fe LDH for ARD.

Keywords: M-Fe layered double hydroxides (LDH); Separation; Alizarin red dye; Pseudo-second-order kinetic models

1. Introduction

Recently, with rapid industrial development, the aquatic environment has suffered from several serious problems. Water pollution has become one of the top environmental problems [1]. One of the most affecting reasons for water contamination is the discharge of dyeing wastewater. These dye contaminants could pollute water streams and groundwater sources as well, causing severe human health problems [2,3]. The discharge of dye contaminants into wastewater is a result of inefficient industrial dyeing processes that may add as much as 15% of unused dyestuff directly to the watercourses [3]. The average concentration levels of effluent-containing dyes normally vary from 10 to 50 mg/L [4,5]. Thus, it may be considered polluted and unacceptable. Alizarin red dye (ARD) or 1,2-dihydroxyanthracene-9,10-dione is the main composition for the madder lake pigments that are commercially known as Rose madder and Alizarin crimson. Alizarin red dye is considered to be one of the most widely used and commercially available dyes in different facilities. ARD is a common type of cationic dye that is usually used in the industry of textile dyeing [6].

ARD has a highly toxic effect on humans, biota, and animals, thus needs to be effectively eliminated from dyeing

* Corresponding author.

wastewater [7]. This exhibits a challenge for the treatment methods to eliminate ARD from wastewater. Different treatment techniques have been applied to deal with wastewater containing dyes, such as ozonation, membrane filtration, reverse osmosis [8], chemical precipitation [9–11], and coagulation [12]. Moreover, the adsorption technique is considered the most effective treatment method for wastewater containing ARD dye. This may be attributed to its simple design, relatively low cost, and high separation efficiency [13,14].

Nowadays, the application of synthetic anionic clays such as layered double hydroxide (LDH) for the treatment of aqueous liquids containing dyes as an effective adsorptive separation technique has attracted great attention [15,16]. These adsorbents exhibited better physicochemical properties, and they are common for the removal of undesirable color, odor, taste, and other organic and inorganic impurities from wastewater owing to their microporous structure, large surface area, and commercial availability. Moreover, such adsorbents are showing higher adsorption capacities and reusability for the removal of organic dyes in different water matrices [17,18]. Consequently, there have been numerous and significant studies conducted on the application of LDH for ARD [18–20]. In this work, we compare the efficiency of both Mg-Fe and Zn-Fe LDH as adsorbent materials for removing ARD. This could be attributed to M-Fe LDH having structured layers, strong performance for ion exchange, a large specific surface area, and a relatively low cost. In this study, co-precipitation with a double titration method was performed to synthesize the M-Fe LDH. This method gave better crystallinity and provided the best control of the particle size [21,22]. The morphological and physical characteristics, besides the structural information of M-Fe LDH were identified via several characterization techniques such as Brunauer–Emmett–Teller (BET), Fourier-transform infrared spectroscopy (FTIR), X-ray diffraction (XRD), and scanning electron microscopy (SEM). The influence of pH, Mg:Fe molar ratio, and M-Fe LDH concentration on the separation of ARD was studied. Besides, the adsorption kinetics, and isotherms were investigated to fit with the M-Fe LDH theory for ARD separation.

The main objectives of this study are to evaluate the adsorptive efficiency of Mg-Fe LDH ligands in the adsorption of ARD and investigate the adsorption kinetics of the applied material throughout the Langmuir and Freundlich adsorption isotherms.

2. Experimental set-up

2.1. Chemical reagents and preparations

In this study, all the chemicals and solvents used were of high analytical grade. In addition, all the solutions were prepared with de-ionized water. The co-precipitation method was used in the preparation of the adsorbent materials. Then we dissolve 2.7 mol of NaOH and 0.9 mol of Na_2CO_3 in 1 L of de-ionized water to prepare the base solution. Then we prepared the metal solution with the same ratios of (4:1) by dissolving 0.09 mol of MCl_2 ($MgCl_2$and $ZnCl_2$) and 0.03 mol of $FeCl_3{\cdot}4H_2O$ into 100 mL of de-ionized water. Then with maintaining the pH in the alkaline media at about 8–10, we add in a drop wise way both base and metal solutions to about 20 mL of de-ionized water. The filtration process was carried out and the filtrate was washed out with excess water. The obtained sample was dried in the oven at about 350 K for 24 h. These prepared samples were known as M-Fe LDH represented in Mg-Fe LDH and Zn-Fe LDH.

2.2. Adsorption studies

The adsorption efficiency of M-Fe LDH could be investigated for the enhanced separation of ARD (100 mL) 20 mg/L at room temperature throughout a series of batch experiments that were carried out under varying the adsorption factors as follows; molar ratios of M (Mg and Zn):Fe (from 1:1–4:1), M-Fe LDH adsorbent dosage (from 0.3–2.1 g/L), initial concentration of ARD (from 5–100 mg/L), contact time intervals (5–120 min) and pH of the solution (from 2 to 10) The pH values were determined by using a pH meter and adjusting 0.1 mol/L HCl and 0.1 mol/L NaOH solutions.

2.3. Adsorption kinetics and characterization

In this work, every batch of experiments was run with both blank samples containing no dye and another containing ARD dye. All experiments were carried out in duplicate, and the average values were obtained for evaluation.

The used adsorbents of M-Fe LDH were characterized before and after the adsorption of ARD by the XRD technique to determine the crystal structures. The crystallinity of the adsorbents could be investigated via PANalytical (Empyrean) X-ray diffraction using Cu Kα radiation (wavelength 1.54060 A^0), with an accelerating voltage of 40 kV, scan angle range from 10° to 60°, step scan of 0.05° and a used current of 30 mA. The vibrations of chemical bonds were determined via the instrument of FTIR spectroscopy by using Bruker (Vertex 70 FTIR-FT Raman) Germany spectrophotometry with a frequency covering a range of 400–4,000 cm^{-1} with serial number 1341 and using a disc of potassium bromide. A high-resolution transmission electron microscope (HRTEM, JEOL-JEM 2100) was used to examine the microstructure of adsorbents. The morphology of the adsorbent material was characterized through field-emission scanning electron microscopy. The BET was used to determine the specific surface area, specific pore volume, and pore sizes of the adsorbent materials through the cumulative adsorption of nitrogen at 77 K using a Micromeritics 2000 instrument [23,24].

The q_e (mg/g) is the adsorption that was calculated using Eq. (1):

$$q_e = \frac{\left(C_0 - C_e\right)V}{m} \tag{1}$$

where C_0 (mg/L) is the ARD initial concentrations, C_e (mg/L) is the ARD equilibrium concentrations, V (L) is the total volume, and m (g) is the mass of the adsorbent M-Fe LDH.

3. Results and discussion

3.1. Effect of M (Mg and Zn):Fe molar ratio on the separation of ARD

The separation efficiency of ARD was increased by increasing the M:Fe molar ratio from 1:1 to 4:1, then lowered by increasing the molar ratio of M:Fe from 4:1 to 6:1 at pH 6.2 as represented in Fig. 1. This may be because when the molar ratio of M/Fe is lower than 4, the adsorption capacity of ARD on M-Fe LDH is restricted to the electrostatic interaction on the adsorbent surface assuming the existence of strong interactions between the layers carrying charges in LDH of high charge densities [25,26]. These charge interactions lower the ability of the LDH to be expanded and accommodate a large number of anions within the interlayer region of LDH. Whereas, when the molar ratio of M/Fe equals 4, the adsorption capacity of M-Fe LDH for ARD will include both the electrostatic adsorption of the most outer layer cations and the exchange adsorption of the interlayer anions. This finding is attributed to the fact that M-Fe LDH (M/Al = 4) has the best crystalline structure of LDH [27]. This structure could increase the uptake ability of the additional species to be up-taken or adsorbed within the LDH interlayers and consequently lead to the highest adsorption affinity for ARD [28]. While, at M-Fe LDH (M/Fe) synthesized molar ratios higher than 4 (5 and 6), certain amounts of amorphous metal hydroxides might be contained in the LDH structure, which could strongly reduce the adsorption efficiency of M-Fe LDH [29]. The achieved separation efficiencies of M (Mg and Zn)/Fe with a molar ratio of 4:1, which is the optimum molar ratio of M/Fe to wipe off ARD, were about 84% and 60% for Mg-Fe LDH and Zn-Fe LDH, respectively.

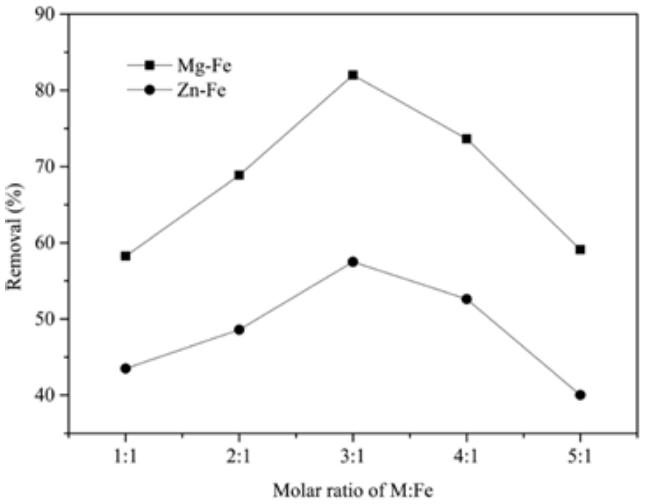

Fig. 1. Effect of the molar ratio of both adsorbents M (Mg and Zn):Fe molar on the removal of ARD.

The physical characteristics and morphological structure of M-Fe LDH at the molar ratio of (4:1) were studied via different characterizing techniques such as FTIR, XRD, BET, and SEM. The morphological structure of both M-(Mg and Zn)-Fe was studied using the SEM technique, which showed that the surface of Mg-Fe LDH has a much larger flocs distribution, more staggered pores, and a more rough texture than that of Zn-Fe LDH (Fig. 2a and b). At the same time, the N_2-BET technique was used to determine the particle size and the specific surface area of both M-Fe LDH which indicated that Mg-Fe LDH has a bigger pore size and a larger surface area than that of Zn-Fe LDH. Where, the calculated specific surface areas were 105.21 and 22.13 m^2/g, for Mg-Fe LDH and Zn-Fe LDH, respectively. These results confirmed that Mg-Fe LDH has a favorable and greater absorptivity for ARD than that of Zn-Fe LDH.

Since the adsorbent chemical structure is of great importance in interpreting the adsorption process. The spectrum of the FTIR technique is an essential tool to identify the functional groups' characteristics [29,30]. The functional groups and the corresponding infrared adsorption bands before and after adsorption on the M-Fe LDH are shown in Fig. 3. Several adsorption peaks were detected throughout the spectrum display, indicating that M-Fe LDH has several active functional groups. The FTIR spectrum for both M-Fe LDH revealed a broad band near 3,500 cm^{-1} that may be related to the vibrational stretching of hydrogen-bonded hydroxyl groups of the water layers and interlayer [30]. Mg-Fe LDH and Zn-Fe LDH are shown in Fig. 3. Besides, sharp bands were detected around 1,450 and 1,650 cm^{-1}

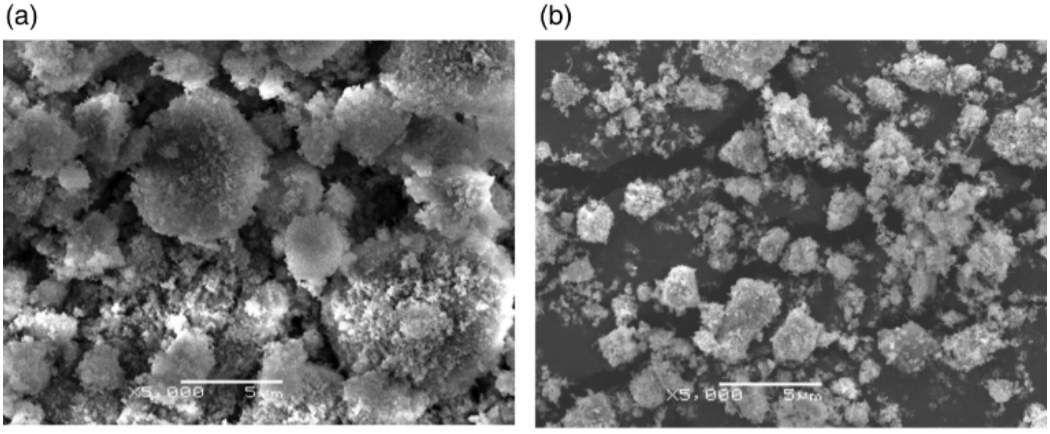

Fig. 2. Scanning electron microscopy image of both M-Fe LDH adsorbents: (a) Mg-Fe LDH and (b) Zn-Fe LDH.

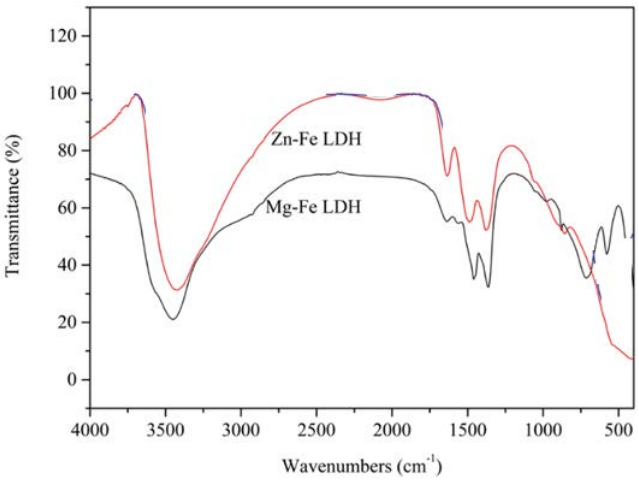

Fig. 3. Fourier-transform infrared spectrum of both adsorbents Mg-Fe LDH and Zn-Fe LDH.

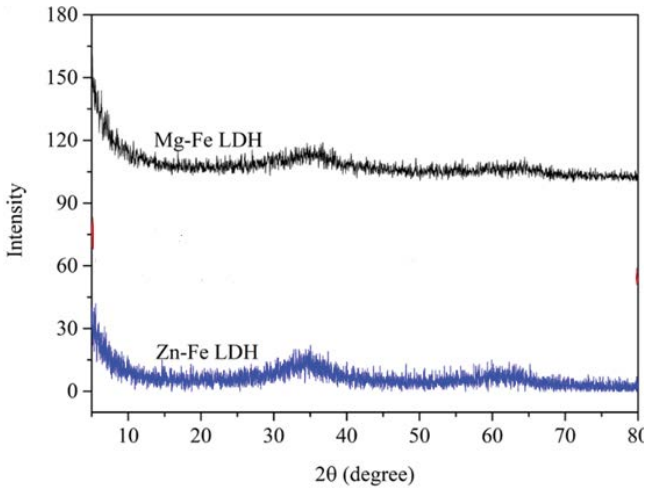

Fig. 4. X-ray diffraction of both adsorbents Mg-Fe LDH and Zn-Fe LDH at dosage molar ratio of (M:Fe = 4:1).

investigated symmetric and asymmetric stretching vibrations of the carboxyl (C=O) group. These detected characteristics were identical for layered double hydroxide (LDH) materials [31]. The detected bands below 1,000 cm^{-1} could be related to metal-oxygen stretching, and metal-hydrogen bonding. The crystallinity and phase information of both adsorbents M (Mg and Zn)-Fe LDH could be detected via XRD. The XRD patterns investigated that both synthesized Mg-Fe LDH and Zn-Fe LDH have very similar crystalline structures under the same conditions, as shown in Fig. 4.

3.2. Effect of M-Fe LDH dosage

The effect of M-Fe LDH dosage at a molar ratio of (M:Fe = 4:1) on the separation efficiency of 20 mg/L of ARD is shown in Fig. 4. The obtained results indicated that by increasing the concentration of M-Fe LDH from 0.3 to 2.1 g/L, the separation efficiency of ARD increased. This may be attributed to the adsorbent dose increasing the number of active sites on the adsorbent surface, enhancing the ability of more ARD to be adsorbed on the surface of the adsorbent, resulting in increasing the separation efficiency of the M-Fe LDH. Whereas, with increasing the M-Fe LDH concentration between 2.1 and 2.7 g/L the ARD separation efficiency was almost maintained constant. The highest achieved separation efficiencies were about 82% and 54% for Mg-Fe LDH, and Zn-Fe LDH, respectively. This may be because, as the adsorbent dosage increases, the rate of collision between particles increases, particle aggregation increases forming a larger particle size, and then the separation efficiency increases. These results were consistent with [32,33]. Hence, the investigated optimum adsorbent (M-Fe LDH) dosage for the ARD separation was determined at 2.1 g/L, which could be applied for the other subsequent experiments.

3.3. Effect of pH on the separation of ARD

Since the pH of an aqueous solution can affect the surface charge of the adsorbents as well as the ionization degree and speciation of different contaminants [31]. The influence

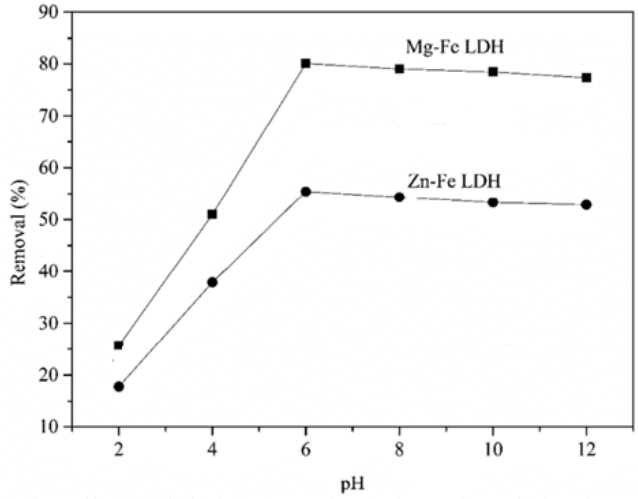

Fig. 5. Effect of pH on the removal of ARD.

of pH solution on the removal of ARD by M-Fe LDH was studied over a pH range of 2–12. Fig. 5 shows the effect of pH on the separation efficiency of ARD (20 mg/L). This effect has been studied using 2.1 g/L M-Fe LDH at room temperature for 30 min. The removal percentage of ARD increased steadily up to pH 6, and behind that, the removal percentage showed relatively unchanged values. This behavior can be explained by the fact that the solution pH can affect both the surface charge of the M-Fe LDH and the ARD molecular nature (cationic molecule) in the solution as well [33]. The obtained results indicated that the maximum separation efficiency of ARD was achieved at pH 6.0, which is slightly acidic and very close to the natural ARD solution's of pH (6.3). Where, at lower pH (pH < 6.0), H^+ was pumped in excess making the adsorbent surface positively charged. Then an adsorption completion was produced between H^+ and the positively charged ARD. So, the rate of ARD separation decreased at a lower pH. At higher pH values (pH > 6.0) the produced negatively charged OH^- and positively charged

ARD react together forming a precipitate. Thus, all other subsequent experiments to study the adsorption variables for ARD separation efficiencies were carried out at pH 6.0.

3.4. Adsorption kinetics

The contact time (t) between the contaminant (ARD) and the adsorbent (M-Fe LDH) is considered an important factor in the adsorption process. The effect of contact time on the separation efficiency of M-Fe LDH for 20 mg/L ARD at room temperature could be shown in Fig. 6. At the beginning of contact time, the rate of ARD adsorption increased rapidly, this may be attributed to the availability of large numbers of active adsorption sites at the adsorbent surface. After a time, the adsorption rate of ARD reached an equilibrium state because the available number of adsorption active sites was lowered. As time progressed, the adsorption process was limited to the rate of ARD transferred from the outer to the inner surface sites of the adsorbents until the full occupation of all available active sites [34,35]. The obtained results confirmed that Mg-Fe LDH had a much higher adsorption capacity for ARD than that obtained from Zn-Fe LDH. In this study, [Eq. (2)] the pseudo-second-order equation was applied to interpret the adsorption kinetics of ARD on the surface of M-Fe LDH adsorbents [36]. The relation between the adsorption capacities vs. time is represented in Fig. 7. Moreover, the other corresponding kinetic parameters are listed in Table 1. The obtained values of R^2 (>0.999) investigated that the adsorption rate of M-Fe LDH for ARD was best fitted with the model of pseudo-second-order. The equilibrium adsorption capacity values achieved in the experiments were in agreement with the calculated pseudo-second-order kinetic values. These results were matched with [37,38].

$$\frac{t}{q_t} = \frac{1}{kq_e^2} + \frac{t}{q_e} \tag{2}$$

where k is the constant of adsorption rate (g/mg·min), q_t (mg/g), q_e (mg/g), and t (min) is time are the adsorption capacities at equilibrium at the time t.

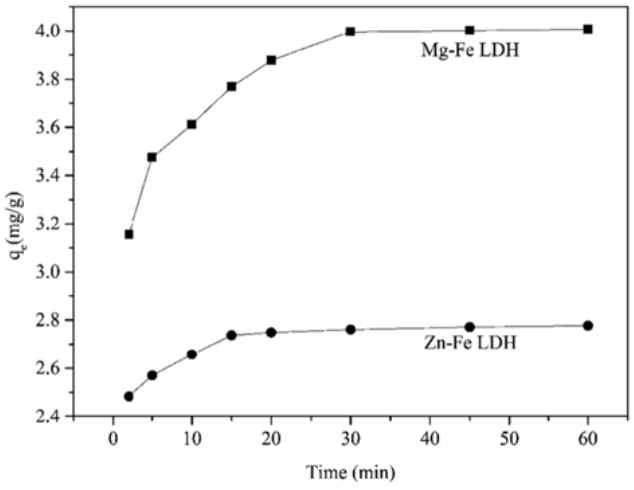

Fig. 6. Effect of contact time on the removal of ARD.

3.5. Adsorption isotherms

The main target of the work is to investigate the maximum adsorption capacity of M (Mg and Zn)-Fe LDH adsorbents for the separation of ARD from wastewater. The adsorption isotherms can be predicted via the two-parameter adsorption isotherms of Langmuir and Freundlich that are usually applied to fit the adsorption capacities of given materials [39]. Where Langmuir isotherm was mostly applied for the description of the monolayer surface homogeneous adsorption as represented in the following equation:

$$\frac{C_e}{q_e} = \frac{C_e}{q_m} + \frac{1}{K_L q_m} \tag{3}$$

where C_e is the concentration of ARD after adsorption equilibrium, q_e is the capacity of adsorption equilibrium, K_L is the adsorption constant and q_m is the maximum adsorption capacity.

Whereas Freundlich isotherm was applied to describe the adsorption on heterogeneous surfaces according to the following equation:

$$\log q_e = \frac{1}{n}\log C_e + \log K_f \tag{4}$$

where n is the adsorption constant and K_f is the Freundlich constant.

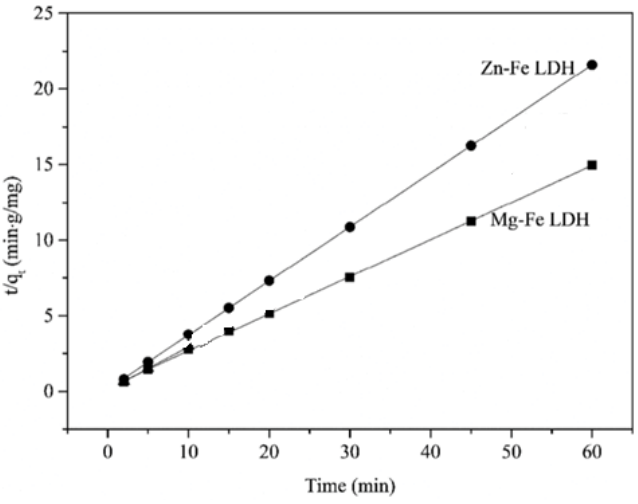

Fig. 7. Pseudo-second-order plot representing the removal of ARD.

Table 1
Parameters of the pseudo-second-order kinetic models

Adsorbents	Concentration of ARD (mg/L)	k	q_e^{cal} (mg/g)	q_e^{exp} (mg/g)	R^2
Mg-Fe LDH	20	0.265	4.1031	4.012	0.99993
Zn-Fe LDH	20	0.901	2.823	3.172	0.99998

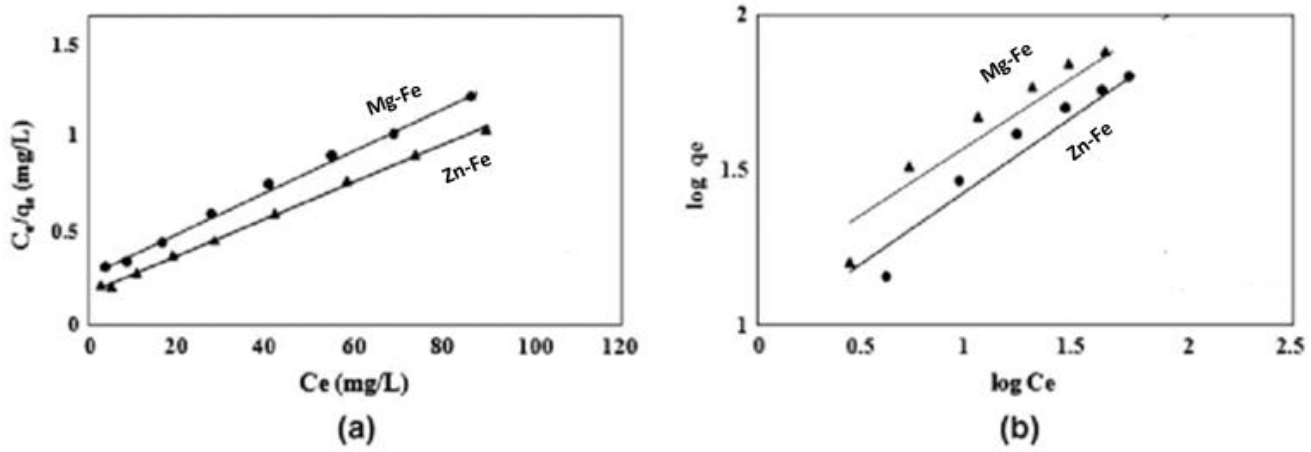

Fig. 8. Linear plots of isothermal models for adsorption of ARD: (a) Langmuir and (b) Freundlich.

Table 2
Parameters of the Langmuir and Freundlich adsorption isotherms

Adsorbent	Langmuir isothermal model			Freundlich isothermal model		
	q_m	K_L	R^2	n	K_f	R^2
Mg-Fe LDH	72.362	0.234	0.995	1.632	3.027	0.986
Zn-Fe LDH	33.753	0.021	0.993	1.670	1.343	0.964

The parameters of both Langmuir and Freundlich adsorption isotherms are shown in Table 2. The linear plots of such adsorption isotherms were represented in Fig. 8a and b as well. The obtained results showed that the Langmuir adsorption isotherm correlation coefficient and R^2 were higher than those obtained from the Freundlich model, which proved the Langmuir adsorption isotherms were more favorable to interpreting the adsorption process of ARD by using M-Fe LDH adsorbent. As a result, the Langmuir adsorption isotherms referred to the uniformity and homogeneous distribution of the active sites on the adsorbent surface and consequently, the adsorption process was monolayer adsorption [40–42]. By comparing the q_m values for ARD of Mg-Fe LDH and Zn-Fe LDH adsorbents we obtained that Mg-Fe LDH had a significantly higher adsorption capacity of 72.362 mg/g than that obtained from Zn-Fe LDH of (33. 753). These results indicated that Mg-Fe LDH was a better adsorbent than Zn-Fe LDH for ARD.

4. Conclusions

In this work, the M (Mg and Zn)-Fe, layered double hydroxides were prepared using the co-precipitation method as efficient adsorbents for the separation of ARD. The ratio of M (Mg and Zn):Fe was 4:1 as an optimal molar ratio for the enhanced separation of ARD. The obtained results investigated the effective dose of M-Fe LDH (2.1 g/L) for the separation of ARD (20 mg/L) was the best at pH 6.0. The kinetic study applied for the adsorption separation of ARD on M-Fe LDH is represented by the pseudo-second-order kinetic model. The achieved results of both adsorbents of M-Fe LDH proved that a Langmuir adsorption isotherm was best fitted. Where the maximum adsorption capacities (q_m) of both adsorbents Mg-Fe LDH and Zn-Fe LDH were 72.4 and 33.8 mg/g, respectively. These results indicated that Mg-Fe LDH could be considered a promising and effective adsorbent material for ARD-enhanced separation from aqueous liquids.

Data availability

The datasets used and/or analyzed during the current study are available from the corresponding author on reasonable request.

References

[1] C. Yang, H. Huang, T. Ji, K. Zhang, L. Yuan, C. Zhou, K. Tang, J. Yi, X. Chen, A cost-effective crosslinked β-cyclodextrin polymer for the rapid and efficient removal of micropollutants from wastewater, Polym. Int., 68 (2019) 805–811.
[2] T. Pan, Z. Li, D. Shou, W. Shou, J. Fan, X. Liu, Y. Liu, Buoyancy assisted Janus membrane preparation by ZnO interfacial deposition for water pollution treatment and self-cleaning, Adv. Mater. Interfaces., 6 (2019) 1901130, doi: 10.1002/admi.201901130.
[3] Z. Liang, J. Wang, Y. Zhang, C. Han, S. Ma, J. Chen, G. Li, T. An, Removal of volatile organic compounds (VOCs) emitted from a textile dyeing wastewater treatment plant and the attenuation of respiratory health risks using a pilot-scale biofilter, J. Cleaner Prod., 253 (2020) 120019, doi: 10.1016/j.jclepro.2020.120019.
[4] H. Langhals, Color Chemistry: Synthesis, Properties and Applications of Organic Dyes and Pigments, Wiley-VCH, Weinheim, 2004.
[5] N.K. Lazaridis, T.D. Karapantsios, D. Georgantas, Kinetic analysis for the removal of a reactive dye from aqueous solution onto hydrotalcite by adsorption, Water Res., 37 (2003) 3023–3033.
[6] Y. Li, Y. Zhang, Y. Zhang, G. Wang, S. Li, R. Han, W. Wei, Reed biochar supported hydroxyapatite nanocomposite: characterization and reactivity for methylene blue removal from aqueous media, J. Mol. Liq., 263 (2018) 53–63.
[7] T.H. Tran, A.H. Le, T.H. Pham, D.T. Nguyen, S.W. Chang, W.J. Chung, D.D. Nguyen, Adsorption isotherms and kinetic modeling of methylene blue dye onto a carbonaceous hydrochar adsorbent derived from coffee husk waste, Sci. Total Environ., 725 (2020) 138325, doi: 10.1016/j.scitotenv.2020.138325.

[8] A.G. Khorram, N. Fallah, Treatment of textile dyeing factory wastewater by electrocoagulation with low sludge settling time: optimization of operating parameters by RSM, J. Environ. Chem. Eng., 6 (2018) 635–642.
[9] H. Ahmed, M. Fawzy, H. Nassar, Effective chemical coagulation treatment process for cationic and anionic dyes degradation, Egypt. J. Chem., 65 (2022) 299–307.
[10] E. Hu, X. Wu, S. Shang, X. Tao, S. Jiang, L. Gan, Catalytic ozonation of simulated textile dyeing wastewater using mesoporous carbon aerogel supported copper oxide catalyst, J. Cleaner Prod., 112 (2016) 4710–4718.
[11] H.R. Rashidi, N.M.N. Sulaiman, N.A. Hashim, C.R.C. Hassan, M.R. Ramli, Synthetic reactive dye wastewater treatment by using nano-membrane filtration, Desal. Water Treat., 55 (2014) 86–95.
[12] H.-J. Lee, M.A. Halali, S. Sarathy, C.-F. de Lannoy, The impact of monochloramines and dichloramines on reverse osmosis membranes in wastewater potable reuse process trains: a pilot-scale study, Environ. Sci. Water Res. Technol., 6 (2020) 1336–1346.
[13] E. Altıntıg, H. Altundag, M. Tuzen, A. Sarı, Effective removal of methylene blue from aqueous solutions using magnetic loaded activated carbon as novel adsorbent, Chem. Eng. Res. Des., 122 (2017) 151–163.
[14] Md. A. Islam, S. Sabar, A. Benhouria, W.A. Khanday, M. Asif, B.H. Hameed, Nanoporous activated carbon prepared from karanj (*Pongamia pinnata*) fruit hulls for methylene blue adsorption, J. Taiwan. Inst. Chem. Eng., 74 (2017) 96–104.
[15] C.-H. Zhou, J.N. Beltramini, C.-X. Lin, Z.-P. Xu, G.Q. (Max) Lu, A. Tanksale, Selective oxidation of biorenewable glycerol with molecular oxygen over Cu-containing layered double hydroxide-based catalysts, Catal. Sci. Technol., 1 (2011) 111–122.
[16] M. Lan, G. Fan, L. Yang, F. Li, Significantly enhanced visible-light-induced photocatalytic performance of hybrid Zn-Cr layered double hydroxide/graphene nanocomposite and the mechanism study, Ind. Eng. Chem. Res., 53 (2014) 12943–12952.
[17] P. Roy Chowdhury, K.G. Bhattacharyya, Ni/Ti layered double hydroxide: synthesis, characterization and application as a photocatalyst for visible light degradation of aqueous methylene blue, Dalton Trans., 44 (2015) 6809–6824.
[18] Y.H. Chuang, Y.M. Tzou, M.K. Wang, C.H. Liu, P.N. Chiang, Removal of 2-chlorophenol from aqueous solution by Mg/Al layered double hydroxide (LDH) and modified LDH, Ind. Eng. Chem. Res., 47 (2008) 3813–3819.
[19] Q. Wang, J.P. Undrell, Y. Gao, G. Cai, J.-C. Buffet, C.A. Wilkie, D. O'Hare, Synthesis of flame-retardant polypropylene/LDH-borate nanocomposites, Macromolecules, 46 (2013) 6145–6150.
[20] E.N. Kalali, X. Wang, D.-Y. Wang, Synthesis of a Fe_3O_4 nanosphere@Mg-Al layered-double-hydroxide hybrid and application in the fabrication of multifunctional epoxy nanocomposites, Ind. Eng. Chem. Res., 55 (2016) 6634–6642.
[21] J. Yu, B.R. Martin, A. Clearfield, Z. Luo, L. Sun, One-step direct synthesis of layered double hydroxide single-layer nanosheets, Nanoscale, 7 (2015) 9448–9451.
[22] M.V. Bukhtiyarova, A review on effect of synthesis conditions on the formation of layered double hydroxides, J. Solid State Chem., 269 (2019) 494–506.
[23] B. Bi, L. Xu, B. Xu, X. Liu, Heteropoly blue-intercalated layered double hydroxides for cationic dye removal from aqueous media, Appl. Clay Sci., 54 (2011) 242–247.
[24] C.M. Futalan, J. Kim, J.-J. Yee, Adsorptive treatment via simultaneous removal of copper, lead and zinc from soil washing wastewater using spent coffee grounds, Water Sci. Technol., 76 (2019) 1029–1041.
[25] R. Chitrakar, A. Sonoda, Y. Makita, T. Hirotsu, Calcined Mg-Al layered double hydroxides for uptake of trace levels of bromate from aqueous solution, Ind. Eng. Chem. Res., 50 (2011) 9280–9285.
[26] R. Chitrakar, A. Sonoda, Y. Makita, T. Hirotsu, A new method for synthesis of Mg-Al, Mg-Fe, and Zn-Al layered double hydroxides and their uptake properties of bromide ion, Ind. Eng. Chem. Res., 47 (2008) 4905–4908.
[27] K.H. Goh, T.T. Lim, Z. Dong, Application of layered double hydroxides for removal of oxyanions: a review, Water Res., 42 (2008) 1343–1368.
[28] T. Riu, R. Linag, M. Wei, D. Evans, X. Duan, Applications of layered double hydroxides, Adv. Funct. Mater., 28 (2018) 1802943.
[29] Y. Wang, H. Gao, Compositional and structural control on anion sorption capability of layered double hydroxides (LDHs), J. Colloid Interface Sci., 301 (2006) 19–26.
[30] J.M. Fernández, M.A. Ulibarri, F.M. Labajos, V. Rives, The effect of iron on the crystalline phases formed upon thermal decomposition of Mg-Al-Fe hydrotalcites, J. Mater. Chem., 8 (1998) 2507–2514.
[31] F. Cavani, F. Trifirò, A. Vaccari, Hydrotalcite-type anionic clays: preparation, properties and applications, Catal. Today, 11 (1991) 173–301.
[32] N. Benselka-Hadj Abdelkader, A. Bentouami, Z. Derriche, N. Bettahar, L.C. de Ménorval, Synthesis and characterization of Mg-Fe layer double hydroxides and its application on adsorption of Orange G from aqueous solution, J. Chem. Eng., 169 (2011) 231–238.
[33] S.-J. Xia, F.-X. Liu, Z.-M. Ni, W. Shi, J.-L. Xue, P.-P. Qian, Ti-based layered double hydroxides: efficient photocatalysts for azo dyes degradation under visible light, Appl. Catal., B, 144 (2014) 570–579.
[34] N. Kannan, M.M. Sundaram, Kinetics and mechanism of removal of methylene blue by adsorption on various carbons a comparative study, Dyes Pigm., 51 (2001) 25–40.
[35] N.K. Amin, Removal of reactive dye from aqueous solutions by adsorption onto activated carbons prepared from sugarcane bagasse pith, Desalination, 223 (2008) 152–161.
[36] S. Rengaraj, Y. Kim, C.K. Joo, J. Yi, Removal of copper from aqueous solution by aminated and protonated mesoporous aluminas: kinetics and equilibrium, J. Colloid Interface Sci., 273 (2004) 14–21.
[37] J. Li, Q. Wang, L. Zheng, H. Liu, A novel graphene aerogel synthesized from cellulose with high performance for removing MB in water, J. Mater. Sci. Technol., 41 (2020) 68–75.
[38] M.E. Fawzy, N.M. Badr, S.I. Abou-Elela, Remediation and reuse of retting flax wastewater using activated sludge process followed by adsorption on activated carbon, J. Environ. Sci. Technol., 11 (2018) 167–174.
[39] H.-J. Choi, Use of methyl esterified eggshell membrane for treatment of aqueous solutions contaminated with anionic sulfur dye, Water Sci. Technol., 76 (2017) 2638–2646.
[40] Y. Xie, G. Ye, S. Peng, S. Jiang, Y. Wang, X. Hu, Postsynthetic functionalization of water stable zirconium metal organic frameworks for high performance copper removal, Analyst, 144 (2019) 4552–4558.
[41] J. Zhao, Q. Huang, M. Liu, Y. Dai, J. Chen, H. Huang, Y. Wen, X. Zhu, X. Zhang, Y. Wei, Synthesis of functionalized MgAl-layered double hydroxides via modified mussel inspired chemistry and their application in organic dye adsorption, J. Colloid Interface Sci., 505 (2017) 168–177.
[42] M.E. Fawzy, H.M. Ahmed, H.F. Nassar, Chicken bone ash as a cost-effective and efficient adsorbent for phenol removal from aqueous solution, Desal. Water Treat., 281 (2023) 255–264.